Journal of Solid State Chemistry **143,** 151–162 (1999)
Article ID jssc.1998.8049, available online at http://www.idealibrary.com on IDEAL®

$ALn_{1\pm x}Bi_{4\pm x}S_8$ (A = K, Rb; Ln = La, Ce, Pr, Nd): New Semiconducting Quaternary Bismuth Sulfides

Lykourgos Iordanidis,* Jon L. Schindler,† Carl R. Kannewurf,† and Mercouri G. Kanatzidis*

*Department of Chemistry and Center for Fundamental Materials Research, Michigan State University, East Lansing, Michigan 48824; and
†Department of Electrical Engineering and Computer Science, Northwestern University, Evanston, Illinois 60208

Received February 14, 1998; in revised form September 24, 1998; accepted September 25, 1998

The isostructural compounds $KLa_{1.28}Bi_{3.72}S_8$ (I), $RbLa_{1\pm x}Bi_{4\pm x}S_8$ (II), $RbCe_{0.84}Bi_{4.16}S_8$ (III), $KCe_{1\pm x}Bi_{4\pm x}S_8$ (IV), $KPr_{1\pm x}B_{4\pm x}S_8$ (V) and $KNd_{1\pm x}Bi_{4\pm x}S_8$ (VI) were synthesized. The structures of compounds (I) and (III) were determined by single crystal X-ray diffraction. They crystallize in the orthorhombic *Pnma* space group (#62), $a = 16.6524(9)$ Å, $b = 4.0712(2)$ Å, $c = 21.589(1)$ Å, $R1 = 0.0397$, $wR2 = 0.0743$ (all data) for (I) and $a = 16.7469(2)$ Å, $b = 4.0528(1)$ Å, $c = 21.753(1)$ Å, $R1 = 0.0345$, $wR2 = 0.0613$ (all data) for (III). The structure type found in these compounds is made up of NaCl-type and Gd_2S_3-type fragments which connect to form tunnels filled with alkali metal ions. The structure has three types of metal positions, a six-coordinate type and two with higher coordination numbers, seven and eight. The NaCl-type fragment contains the six-coordinate positions which are exclusively occupied by Bi atoms, while the Gd_2S_3-type fragment contains the seven- and eight-coordinate positions which display mixed bismuth/lanthanide atom occupancy. The compounds are semiconductors with band gaps around 1.0 eV and they melt incongruently between 770 and 800°C. The electrical conductivities of the La analogs and magnetic properties of the Ce analogs are reported.

INTRODUCTION

Bismuth compounds constitute a great part of the naturally occurring sulfosalts. These minerals exhibit a staggering compositional complexity and structural diversity (1), partly due to the Bi $6s^2$ lone pair which can be stereochemically expressed, leading to a distorted local coordination for the Bi atom. Alternatively, the lone pair can be totally stereochemically inactive to produce a regular octahedral Bi^{3+} center. Almost any intermediate stage in the continuum which exists between full stereochemical expression and complete suppression of the $6s^2$ lone pair via sp^3d^2 hybridization is observed. This property gives rise to what may very well be the most malleable coordination geometry in the periodic table. Therefore, from a coordination as well as a solid state chemistry perspective, it is interesting to study the behavior of Bi^{3+} and its role in stabilizing various structure types. Furthermore, interest in multinary Bi chalcogenides compounds is growing due to their potential relevance in thermoelectric applications (2). It is noteworthy that $Bi_{2-x}Sb_xTe_{3-y}Se_y$ alloys are currently the best thermoelectric materials (3) for room temperature cooling applications.

In the past 20 years several synthetic Bi ternary compounds with alkali metals have been structurally characterized: $ABiQ_2$ (A = alkali metal; Q = chalcogen) (4), $CsBi_3S_5$ (5), $RbBi_3S_5$ (6), $Cs_3Bi_7Se_{12}$ (7), α-,β-$BaBi_2S_4$ (8), $Sr_4Bi_6Se_{13}$ (9), $BaBiSe_3$ (10). Only recently have several new ternary compounds been synthesized, such as β-,γ-$CsBiS_2$ (11), KBi_3S_5 (12), $KBi_{6.33}S_{10}$ (13), $K_2Bi_8S_{13}$ (13), α-$K_2Bi_8Se_{13}$ (11), β-$K_2Bi_8Se_{13}$ (14), $K_{2.5}Bi_{8.5}Se_{14}$ (14), $BaBiTe_3$ (15), $RbBi_4Se_7$ (16a), $A_2Bi_8Se_{13}$ (A = Rb, Cs) (16a), $CdBi_2S_4$ (17), $CdBi_4S_7$ (17), $Cd_{2.8}Bi_{8.1}S_{15}$ (17), and $Cd_2Bi_6S_{11}$ (17). Some of these compounds possess promising thermoelectric properties (2, 14, 15, 18). Much remains to be learned, however, about the chemistry and properties of these structurally complicated systems.

The incorporation of large electropositive ions such as lanthanides (Ln) into bismuth chalcogenide frameworks is expected to lead to materials with low thermal conductivity, due to the high coordination sites these ions adopt and the ionic character of the surrounding Ln–Q bonds (18). Only a limited number of ternary lanthanide compounds are known so far, including $EuBi_2S_4$ (19), Eu_2BiS_4 (20), $La_4Bi_2S_9$ (21), $Ce_{1.25}Bi_{3.78}S_8$ (22), $Eu_3Bi_4Q_9$ (Q = S, Se) (23), and these compounds are little studied. Even less is known about quaternary lanthanide bismuth chalcogenides. In the ternary compounds the Bi atom most often occupies an octahedral (often distorted) coordination but it can also occupy higher coordination sites. Given the high effective ionic radius in these high coordination sites and the similarity of the size of Bi^{3+} to the sizes of several Ln^{3+} ions, we became interested in Bi^{3+}/Ln^{3+} substitution chemistry in such sites. Because of the very different valence orbital energies of Ln^{3+} and Bi^{3+} centers, the incorporation of lanthanide ions into a Bi–Q framework could dramatically

0022-4596/99 $30.00

affect the electronic properties of that framework. For these reasons we decided to explore the solid state chemistry of the *A*–*Ln*–Bi–*Q* systems (*A* = alkali or alkaline earth metal; *M* = lanthanide metal; *Q* = S, Se). We have already reported on $BaLaBi_2Q_6$ (24) (*Q* = S, Se), which possesses a tunnel structure stabilized by Q_2^{2-} groups. Here we report on the synthesis, physicochemical, spectroscopic, structural, and electrical characterization of the new compounds $ALn_{1\pm x}Bi_{4\pm x}S_8$ (*A* = K, Rb; *Ln* = La, Ce, Pr, Nd). The relationship of these phases with $Ce_{1.25}Bi_{3.78}S_8$ (22) is examined and it is proposed that the latter is in fact a $KCe_{1\pm x}Bi_{4\pm x}S_8$ phase.

EXPERIMENTAL

Synthesis

Chemicals in this work were used as obtained: (i) bismuth powder 99.999 + % purity, − 100 mesh, Cerac, Milwaukee, WI; (ii) cerium powder 99.9% purity, < 250 μm, Alfa Aesar, Ward Hill, MA; (iii) sulfur powder, sublimed, Spectrum Chemical Mfg. Corp., Gardena, CA; (iv) potassium metal granules, 99%, purity, < 6 mm, Aldrich Chemical Co., Inc., Milwaukee, WI; (v) rubidium metal 99.8% purity, Alfa Aesar, Ward Hill, MA; (vi) lanthanum sulfide 99.9% purity, − 200 mesh, Cerac, Milwaukee, WI. K_2S and Rb_2S were prepared by a stoichiometric reaction of the corresponding alkali metal and sulfur in liquid ammonia as described earlier (13). All manipulations were performed under a atmosphere of dry nitrogen using a Vacuum Atmospheres DriLab glovebox.

$KLa_{1.28}Bi_{3.72}S_8$ (**I**)

A mixture of 0.027 g (0.245 mmol) K_2S, 0.500 g (0.972 mmol) Bi_2S_3, and 0.092 g (0.246 mmol) La_2S_3 was transferred to a carbon-coated quartz tube which was flame-sealed under high vacuum (10^{-4}–10^{-5} mbar). The tube was heated for 6 days at 820°C and was cooled to 420°C at 10°C/h and then to 50°C in 10 h. The product consisted of silver-gray needles, several millimeters long, and was isolated by washing with water, methanol, and ether. Semiquantitative energy dispersive spectroscopy (EDS) analysis using a scanning electron microscope (SEM) on a number of needles gave an average composition of $K_{0.9}La_{1.3}Bi_{4.0}S_{8.0}$.

$RbLa_{1\pm x}Bi_{4\pm x}S_8$ (**II**)

A mixture of 0.030 g (0.148 mmol) Rb_2S, 0.304 g (0.591 mmol) Bi_2S_3, and 0.055 g (0.147 mmol) La_2S_3 was transferred to a carbon-coated quartz tube which was flame-sealed under vacuum. The tube was heated for 6 days at 850°C and was cooled to 450°C at 10°C/h and then to 50°C in 10 h. Silver-gray needles were isolated by washing with water, methanol, and ether. Standardless SEM/EDS on a number of needles gave an average composition of $Rb_{0.6}La_{1.1}Bi_{4.3}S_{8.0}$.

$RbCe_{0.84}Bi_{4.16}S_8$ (**III**)

A mixture of 0.050 g (0.246 mmol) Rb_2S, 0.500 g (0.972 mmol) Bi_2S_3, 0.068 g (0.485 mmol) Ce metal, and 0.024 g (0.748 mmol) of elemental S was transferred into a carbon-coated quartz tube, sealed under vacuum, heated at 850°C for 6 days and cooled to 450°C at 10°C/h and then to 50°C in 10 h. The product consisted of a metallic-gray chunk with needles growing on its top. Standardless SEM/EDS analysis gave all four elements with the following ratio: $Rb_{0.6}Ce_{0.9}Bi_{4.6}S_{8.0}$.

$KCe_{1\pm x}Bi_{4\pm x}S_8$ (**IV**)

The procedure was similar to the ones above. A mixture of 0.030 g (0.272 mmol) K_2S, 0.559 g (1.087 mmol) Bi_2S_3, 0.076 g (0.542 mmol) Ce metal, and 0.026 g (0.811 mmol) of elemental S was used. Standardless SEM/EDS analysis gave all four elements with the following ratio: $K_{0.9}Ce_{1.1}Bi_{4.2}S_{8.0}$.

$KPr_{1\pm x}Bi_{4\pm x}S_8$ (**V**) *and* $KNd_{1\pm x}Bi_{4\pm x}S_8$ (**VI**)

The procedure was similar to the ones above. A mixture of 0.016 g (0.145 mmol) K_2S, 0.292 g (0.568 mmol) Bi_2S_3, 0.040 g for Pr (or 0.041 g for Nd) (0.277 mmol) metal, and 0.014 g (0.437 mmol) of elemental S was used. Their elemental compositions were $K_{0.9}Pr_{1.6}Bi_{3.9}S_8$ and $K_{1.7}Nd_{1.4}Bi_{4.2}S_8$, respectively. All compounds are stable in air and water.

PHYSICAL MEASUREMENTS

Electron Microscopy

Quantitative microprobe analyses of the compound were performed with a JEOL JSM-35C SEM equipped with a Tracor Northern EDS detector. Data were acquired using an accelerating voltage of 20 kV and a 1-min accumulation time.

Differential Thermal Analysis

Differential thermal analysis (DTA) was performed with a computer-controlled Shimadzu DTA-50 thermal analyzer. The ground single crystals (~20 mg total mass) were sealed in quartz ampoules under vacuum. A quartz ampoule containing alumina of equal mass was sealed and placed on the reference side of the detector. The samples were heated to the desired temperature at 10°C/min, then isothermed for 5 min, followed by cooling at 10°C/min to 100°C and finally by rapid cooling to room temperature. The reported DTA

temperature is the peak temperature. The DTA samples were examined by powder X-ray diffraction after the experiment.

Solid State UV/Vis Spectroscopy

Optically determined bandgaps were determined as reported elsewhere (25).

Electrical Conductivity Measurements

DC electrical conductivity measurements were made on polycrystalline compactions of the compounds, as reported elsewhere (14, 26).

Magnetic Measurements

The magnetic response of the Ce compounds was measured over the range 2–300 K using an MPMS Quantum Design SQUID magnetometer. Samples were ground to a fine powder to minimize possible anisotropic effects and loaded into PVC containers. The results were corrected for core atom diamagnetism. Magnetization as a function of field strength (at a constant temperature of 5 K) was investigated to determine whether the samples experienced saturation of their magnetic signal. For both compounds magnetization increased linearly with increasing field over the range 100–10,000 G. The subsequent temperature-dependent studies were performed at moderate field strengths (1000–2000 G).

Powder X-ray Crystallography

The compounds were examined by X-ray powder diffraction to check for phase purity and for identification. These powder patterns showed that all phases are isostructural. Powder patterns were obtained using a Rigaku-Denki/Rw400F2 (Rotaflex) rotating-anode powder diffractometer and a CPS 120 INEL X-ray powder diffractometer equipped with a position-sensitive detector. The purity and homogeneity of all phases was confirmed by comparison of X-ray powder diffraction to those calculated from single crystal data using the CERIUS^2 software (27). Table 1 contains the $d_{calc,}$ d_{obs}, and I/I_{max} (obs) for (**I**) together with the d_{obs} and I/I_{max} (obs) for (**II**).

TABLE 1
Calculated and Observed X-Ray Powder Diffraction Patterns for $KLa_{1.28}Bi_{3.72}S_8$ and $RbLa_{1\pm x}Bi_{4\pm x}S_8$

	$KLa_{1.28}Bi_{3.72}S_8$			$RbLa_{1\pm x}Bi_{4\pm x}S_8$	
h k l	d_{calc} (Å)	d_{obs} (Å)	I/I_{max} (obs)	d_{obs} (Å)	I/I_{max} (obs)
1 0 1	13.148	13.123	4	13.301	3
0 0 2	10.755	10.735	5	10.893	2
2 0 0	8.306	8.300	19	8.379	13
2 0 1	7.749	7.742	7	7.810	6
2 0 2	6.574	6.563	22	6.632	9
2 0 3	5.428	5.427	4	5.484	2
3 0 1	5.363	5.359	13	5.397	11
1 0 4	5.116	5.107	3	5.160	1
3 0 3	4.383	4.377	12	4.416	8
1 0 5	4.165	4.160	5	4.205	4
1 1 1	3.874	3.870	2	3.899	3
1 1 2	3.698	3.697	3	3.720	1
4 0 3	3.594	3.589	100	3.619	100
2 1 1	3.592				
0 0 6	3.585				
0 1 3	3.529	3.528	7	3.541	6
2 1 2	3.451	3.446	5	3.473	3
3 0 5	3.397	3.394	13	3.426	9
2 0 6	3.292	3.284	26	3.311	14
5 0 1	3.284				
3 1 1	3.234	3.233	8	3.252	5
1 1 4	3.177	3.174	16	3.193	13
5 0 2	3.174				
3 1 2	3.129	3.125	2	3.148	2
2 1 4	3.016	3.014	16	3.035	13
5 0 3	3.015				
1 1 5	2.905	2.903	9	2.926	7
4 1 0	2.901				
5 0 4	2.826	2.824	3	2.846	3
3 1 4	2.795	2.779	10	2.801	8
2 1 5	2.780				
5 0 5	2.630	2.629	5	2.648	4
6 0 3	2.583	2.582	16	2.598	13
3 1 6	2.416	2.416	6	2.434	3
6 0 5	2.328	2.323	3	2.344	3
3 1 7	2.240	2.237	6	2.254	3
6 1 2	2.236			2.241	2
3 0 9	2.194	2.193	8	2.214	4
6 1 3	2.178	2.176	4	2.188	3
3 1 8	2.077	2.071	13	2.090	12
4 0 9	2.072				
2 0 12	1.752	1.747	8	1.756	6

Single-Crystal X-ray Crystallography

$KLa_{1.28}Bi_{3.72}S_8$ (**I**). A Siemens SMART Platform CCD diffractometer was used for data collection. An initial set of cell constants was calculated from reflections harvested from three sets of 15 frames. These initial sets of frames were oriented such that orthogonal wedges of reciprocal space were surveyed. This produced an orientation matrix determined from 80 reflections. Final cell constants were calculated from a set of 5334 strong reflections obtained from the data collection (Table 2).

The data collection technique used is known as hemisphere collection. Here a region of reciprocal space was surveyed to the extent of 1.3 hemispheres to a resolution of

TABLE 2
Crystallographic Data for $KLa_{1.28}Bi_{3.72}S_8$ and $RbCe_{0.84}Bi_{4.16}S_8$

	Crystal data	
Empirical formula	$KLa_{1.28}Bi_{3.72}S_8$	$RbCe_{0.84}Bi_{4.16}S_8$
Crystal habit, color	Needle, silver	Needle, silver
Crystal size	$0.80 \times 0.05 \times 0.05$ mm	$0.50 \times 0.09 \times 0.15$ mm
Crystal system	Orthorhombic	Orthorhombic
Space group	*Pnma* (#62)	*Pnma* (#62)
	$a = 16.6524(9)$ Å	$a = 16.7469(2)$ Å
	$b = 4.0712(2)$ Å	$b = 4.0528(1)$ Å
	$c = 21.589(1)$ Å	$c = 21.753(1)$ Å
Volume	1463.6(1) Å^3	1476.42(4) Å^3
Z	4	4
Density (calculated)	5.676 g/cm^3	5.981 g/cm^3
Formula weight	1250.79	1329.36
Absorption coefficient	49.617 mm^{-1}	56.366 mm^{-1}
$F(000)$	2115	2237
	Data collection	
Diffractometer	Siemens SMART platform CCD	Siemens SMART platform CCD
Wavelength	0.71073 Å	0.71073 Å
Temperature	293 (2) K	293 (2) K
θ for data collection	1.54 to 27.14°	1.53 to 25.03°
Index ranges	$-18 \le h \le 20$	$-19 \le h \le 19$
	$-5 \le k \le 4$	$-4 \le k \le 4$
	$-26 \le l \le 25$	$-25 \le l \le 25$
Reflections collected	7609	12291
Independent reflections	1734 [R(int) = 0.0507]	1504 [R(int) = 0.0497]
	Solution and refinement	
System used	SHELXTL-V5.0	SHELXTL-V5.0
Solution	Direct methods	Direct methods
Refinement method	Full-matrix least-squares on F^2	Full-matrix least-squares on F^2
Absorption correction	SADABS	SADABS
Max. and min transmission	1.000 and 0.321	1.000 and 0.268
Data/restraints/parameters	1733/0/88	1504/0/88
Goodness-of-fit on F^2	1.068	1.111
Final R indices [$I > 2\sigma(I)$]:	$R1 = 0.0313$	$R1 = 0.0292$
	w$R2 = 0.0677$	w$R2 = 0.0597$
R indices (all data)	$R1 = 0.0397$	$R1 = 0.0345$
	w$R2 = 0.0743$	w$R2 = 0.0613$
Extinction coefficient	0.00123(7)	0.00059(5)
Largest diff. peak and hole	3.077 and -2.077 eÅ^{-3}	2.058 and -1.635 eÅ^{-3}

Note. $R1 = \sum||F_o| - F_c||/|\sum|F_o|$. $wR2 = \{\sum[w(F_o^2 - F_c^2)^2]/\sum[w(F_o^2)^2]\}^{1/2}$.

0.75 Å. Three major swaths of frames were collected with 0.30° steps in ω and an exposure time of 10 s per frame. The SMART (28a) software was used for data acquisition and SAINT (28b) was used for data extraction.

The absorption correction was done using SADABS (28c) and all refinements were done using the SHELXTL (28d) package of crystallographic programs. Four bismuth atoms, one lanthanum, and eight sulfur atoms were found to sit on crystallographic mirror planes (site 4c, x 1/4 z) (Tables 3 and 4). Next to the La(2) site significant electron density was found (18.17 eÅ^{-3}) and the thermal parameter U of Bi(4) was higher (0.025 Å^2) compared to the other bismuth atoms ($\sim$0.012 Å^2, $R1 = 7.1\%$ w$R2 = 17.0\%$). A disorder model was applied for both sites. The electron density close to the La(2) site was assigned as Bi(5) and the sum of the occupancies was constrained equal to 0.500 (fully occupied). The atoms in this site were assigned according to the coordination environments and bond distances with the surrounding sulfur atoms. La(2) has a bicapped trigonal prism coordination with distances varying between 2.940(2) and 3.246(4) Å, while Bi(5) has a square pyramid coordination with distances varying between 2.723(8) and 2.979(4) Å (Table 5). La(1) was introduced also in the Bi(4) site (i.e., a mixed occupancy model was used) and the sum of the occupancies was set

TABLE 3
Atomic Coordinates and Equivalent Isotropic Displacement Parameters ($Å^2 \times 10^3$) for $KLa_{1.28}Bi_{3.72}S_8$

	x	*y*	*z*	*U*(eq)	Occ.
Bi(1)	0.5432(1)	0.2500	0.7426(1)	13(1)	
Bi(2)	0.6510(1)	0.7500	0.8968(1)	12(1)	
Bi(3)	0.4278(1)	0.2500	0.9158(1)	14(1)	
Bi(4)	0.4669(1)	0.7500	0.5928(1)	16(1)	0.550(8)
La(1)	0.4669(1)	0.7500	0.5928(1)	16(1)	0.450
La(2)	0.7066(1)	0.7500	0.5464(1)	8(1)	0.831(6)
Bi(5)	0.7266(4)	0.7500	0.5339(3)	17(2)	0.169
K(1)	0.8017(2)	0.7500	0.7418(1)	18(1)	
S(1)	0.6066(2)	0.7500	0.6755(2)	12(1)	
S(2)	0.4105(2)	0.2500	0.6725(2)	12(1)	
S(3)	0.6886(2)	0.2500	0.8205(2)	13(1)	
S(4)	0.4746(2)	0.7500	0.8317(2)	16(1)	
S(5)	0.7908(2)	0.7500	0.9465(2)	11(1)	
S(6)	0.6165(2)	0.2500	0.9983(2)	13(1)	
S(7)	0.2842(2)	0.2500	0.8757(2)	11(1)	
S(8)	0.5732(2)	0.2500	0.5441(1)	10(1)	

Note. *U*(eq) is defined as one-third of the trace of the orthogonalized U_{ij} tensor.

equal to 0.500 (fully occupied). After refinement the *R*1 and w*R*2 values dropped to 4.8 and 11.3%, respectively. The split La(2) site is occupied by 83% Bi and 17% La, while the Bi(4) site contains 55% Bi and 45% La. All atoms except La(2) and Bi(5) were refined anisotropically ($R1 = 4.0\%$, $wR2 = 7.4\%$). The formula of the compound refined to $KLa_{1.28}Bi_{3.72}S_8$.

TABLE 4
Anisotropic Displacement Parameters ($Å^2 \times 10^3$) for $KLa_{1.28}Bi_{3.72}S_8$

	U_{11}	U_{22}	U_{33}	U_{23}	U_{13}	U_{12}
Bi(1)	14(1)	15(1)	9(1)	0	0(1)	0
Bi(2)	11(1)	18(1)	12(1)	0	0(1)	0
Bi(3)	11(1)	17(1)	8(1)	0	−1(1)	0
Bi(4)	19(1)	15(1)	16(1)	0	2(1)	0
La(1)	19(1)	15(1)	16(1)	0	2(1)	0
K(1)	21(2)	22(2)	13(2)	0	3(1)	0
S(1)	17(2)	17(2)	13(2)	0	5(1)	0
S(2)	13(2)	14(2)	7(2)	0	2(1)	0
S(3)	14(2)	16(2)	7(2)	0	2(1)	0
S(4)	8(2)	19(2)	6(2)	0	−1(1)	0
S(5)	9(2)	17(2)	5(2)	0	2(1)	0
S(6)	7(2)	20(2)	7(2)	0	1(1)	0
S(7)	12(2)	17(2)	7(2)	0	2(1)	0
S(8)	12(2)	20(2)	7(2)	0	2(1)	0

Note. The anisotropic displacement factor exponent takes the form

$$-2\pi^2[h^2a^{*2}U_{11} + k^2b^{*2}U_{22} + l^2c^{*2}U_{33} + 2hka^*b^*U_{12} + 2hla^*c^*U_{13} + 2klb^*c^*U_{23}].$$

TABLE 5
Bond Lengths and Angles for $KLa_{1.28}Bi_{3.72}S_8$

Lengths Å		Angles (°)	
Bi(1)–S(1)	2.713(2) × 2	S(2)–Bi(1)–S(1)	91.11(8)
Bi(1)–S(2)	2.679(3)	S(2)–Bi(1)–S(3)	179.60(9)
Bi(1)–S(3)	2.948(3)	S(4)–Bi(1)–S(4)	84.62(9)
Bi(1)–S(4)	3.024(2) × 2		
Bi(2)–S(3)	2.693(2) × 2	S(5)–Bi(2)–S(3)	92.58(9)
Bi(2)–S(4)	3.257(4)	S(3)–Bi(2)–S(6)	171.65(8)
Bi(2)–S(5)	2.563(3)	S(5)–Bi(2)–S(6)	82.54(8)
Bi(2)–S(6)	3.046(2) × 2	S(6)–Bi(2)–S(4)	98.09(8)
Bi(3)–S(4)	2.837(2) × 2	S(7)–Bi(3)-S(4)	92.32(9)
Bi(3)–S(6)	2.850(2) × 2	S(4)–Bi(3)–S(6)	88.57(7)
Bi(3)–S(6)	3.612(3)	S(7)–Bi(3)–S(6)	170.33(9)
Bi(3)–S(7)	2.542(3)	S(6)–Bi(3)–S(6)	84.49(8)
M(1)–S(1)	2.932(3)		
M(1)–S(2)	2.827(2) × 2		
M(1)–S(8)	2.895(2) × 2		
M(1)–S(5)	3.053(3)		
M(1)–S(8)	3.029(3)		
Bi(5)–La(2)	0.429(6)		
Bi(5)–S(1)	3.652(8)		
Bi(5)–S(5)	2.790(4) × 2		
Bi(5)–S(6)	2.723(8)		
Bi(5)–S(7)	2.979(4) × 2		
Bi(5)–S(8)	3.274(6) × 2		
La(2)–S(1)	3.246(4)		
La(2)–S(5)	2.966(3) × 2		
La(2)–S(6)	3.124(4)		
La(2)–S(7)	2.940(2) × 2		
La(2)–S(8)	3.013(3) × 2		
K–S(1)	3.551(5)		
K–S(2)	3.293(4) × 2		
K–S(3)	3.252(3) × 2		
K–S(4)	3.288(5)		
K–S(7)	3.266(4) × 2		

$RbCe_{0.84}Bi_{4.16}S_8$ (**III**). A Siemens SMART Platform CCD diffractometer was used for data collection. This same technique as above was used for data collection. The exposure time was 30 s per frame. The initial cell was determined from 69 reflections and the final cell was calculated from a set of 8013 reflections from the actual data collection (Table 2). The resolution of the data set is 0.84 Å. The SMART software was used for data acquisition and SAINT was used for data extraction.

After absorption correction with SADABS and refinement with the SHELXTL programs, as in the previous case, four bismuth atoms, one cerium, and eight sulfur atoms were found to sit on a crystallographic mirror plane (site 4c, *x* 1/4 *z*) (Tables 6 and 7). Significant electron density (21.04

TABLE 6
Atomic Coordinates and Equivalent Isotropic Displacement Parameters ($Å^2 \times 10^3$) for $RbCe_{0.84}Bi_{4.16}S_8$

	x	*y*	*z*	*U*(eq)	Occ.
Bi(1)	0.5396(1)	0.2500	0.2598(1)	18(1)	
Bi(2)	0.1465(1)	0.7500	0.3972(1)	17(1)	
Bi(3)	0.4272(1)	0.2500	0.0849(1)	19(1)	
Bi(4)	0.4728(1)	0.7500	0.4100(1)	23(1)	0.702(9)
Ce(1)	0.4728(1)	0.7500	0.4100(1)	23(1)	0.298
Bi(5)	0.2255(4)	0.7500	0.0307(3)	29(1)	0.460(8)
Ce(2)	0.2075(4)	0.7500	0.0433(3)	15(1)	0.540
Rb	0.2984(1)	0.7500	0.2427(1)	21(1)	
S(1)	0.6051(2)	0.7500	0.3251(1)	16(1)	
S(2)	0.4115(2)	0.2500	0.3326(1)	16(1)	
S(3)	0.6819(2)	0.2500	0.1784(1)	18(1)	
S(4)	0.4726(2)	0.7500	0.1682(1)	20(1)	
S(5)	0.2881(2)	0.7500	0.4440(1)	16(1)	
S(6)	0.1156(2)	0.2500	0.4980(1)	18(1)	
S(7)	0.2823(2)	0.2500	0.1190(1)	16(1)	
S(8)	0.5758(2)	0.2500	0.4579(1)	17(1)	

Note. *U*(eq) is defined as one third of the trace of the orthogonalized U_{ij} tensor.

$eÅ^{-3}$) was found close to the Ce(2) site and also the thermal parameter *U* of Bi(4) was higher (0.029 $Å^2$) compared to the other bismuth atoms (~ 0.017 $Å^2$, $R1 = 8.0\%$ w$R2 = 19.8\%$). A disorder model was applied for both sites. The electron density near the Ce(2) site was assigned as Bi(5) and the sum of the occupancies was constrained to be equal to 0.500 (fully occupied). The atoms in this site were assigned according to the coordination environments and bond distances with the surrounding sulfur atoms. Ce(2) has a bicapped trigonal prism coordination with distances varying between 2.897(6) and 3.338(6) Å, while Bi(5) has a square pyramid coordination with distances varying between 2.754(7) and 2.954(5) Å (Table 8). Ce(1) was introduced also in the Bi(4) site and the sum of the occupancies was set equal to 0.500 (fully occupied). After refinement the *R*1 and w*R*2 values dropped to 4.1 and 9.1%, respectively. The split Ce(2) site is occupied by 54% Bi and 46% Ce, while the Bi(4) site contains 70% Bi and 30% Ce. All atoms except Ce(2) and Bi(5) were refined anisotropically ($R1 = 3.5\%$, w$R2 = 6.1\%$). The formula of the compound based on this refinement was $RbCe_{0.84}Bi_{4.16}S_8$.

TABLE 7
Anisotropic Displacement Parameters ($Å^2 \times 10^3$) for $RbCe_{0.84}Bi_{4.16}S_8$

	U_{11}	U_{22}	U_{33}	U_{23}	U_{13}	U_{12}
Bi(1)	19(1)	17(1)	17(1)	0	0(1)	0
Bi(2)	18(1)	17(1)	16(1)	0	1(1)	0
Bi(3)	18(1)	19(1)	19(1)	0	0(1)	0
Bi(4)	28(1)	17(1)	24(1)	0	− 2(1)	0
Ce(1)	28(1)	17(1)	24(1)	0	− 2(1)	0
Rb	22(1)	22(1)	21(1)	0	3(1)	0
S(1)	17(2)	17(2)	16(2)	0	0(1)	0
S(2)	11(2)	20(2)	17(2)	0	− 1(1)	0
S(3)	24(2)	17(2)	12(2)	0	1(1)	0
S(4)	23(2)	20(2)	17(2)	0	− 3(1)	0
S(5)	15(2)	18(2)	15(2)	0	0(1)	0
S(6)	21(2)	18(2)	15(2)	0	2(1)	0
S(7)	16(2)	17(2)	16(2)	0	− 2(1)	0
S(8)	13(2)	23(2)	15(2)	0	− 1(1)	0

Note. The anisotropic displacement factor exponent takes the form

$$-2\pi^2[h^2a^{*2}U_{11} + k^2b^{*2}U_{22} + l^2c^{*2}U_{33} + 2hka^*b^*U_{12} + 2hla^*c^*U_{13} + 2klb^*c^*U_{23}].$$

TABLE 8
Bond Lengths and Angles for $RbCe_{0.84}Bi_{4.16}S_8$

Lengths (Å)		Angles (°)	
Bi(1)–S(1)	2.707(2) × 2	S(2)–Bi(1)–S(1)	90.80(8)
Bi(1)–S(2)	2.667(3)	S(2)–Bi(1)–S(3)	179.89(9)
Bi(1)–S(3)	2.969(3)	S(4)–Bi(1)–S(4)	83.12(8)
Bi(1)–S(4)	3.055(2) × 2		
Bi(2)–S(3)	2.676(2) × 2	S(5)–Bi(2)–S(3)	92.22(9)
Bi(2)–S(4)	3.242(3)	S(3)–Bi(2)–S(6)	171.40(7)
Bi(2)–S(5)	2.580(3)	S(5)–Bi(2)–S(6)	82.60(8)
Bi(2)–S(6)	3.032(2) × 2	S(6)–Bi(2)–S(4)	99.46(8)
Bi(3)–S(4)	2.823(2) × 2	S(7)–Bi(3)–S(4)	94.00(8)
Bi(3)-S(6)	2.862(2) × 2	S(4)–Bi(3)–S(6)	89.03(6)
Bi(3)–S(6)	3.636(3)	S(7)–Bi(3)–S(6)	167.25(8)
Bi(3)–S(7)	2.537(3)	S(6)–Bi(3)–S(6)	83.66(8)
M(1)–S(1)	2.883(3)		
M(1)–S(2)	2.827(2) × 2		
M(1)–S(8)	2.858(2) × 2		
M(1)–S(5)	3.181(3)		
M(1)–S(8)	2.987(3)		
Bi(5)–Ce(2)	0.407(7)		
Bi(5)–S(1)	3.729(6)		
Bi(5)–S(5)	2.778(5) × 2		
Bi(5)–S(6)	2.754(7)		
Bi(5)–S(7)	2.951(5) × 2		
Bi(5)–S(8)	3.233(5) × 2		
Ce(2)–S(1)	3.338(6)		
Ce(2)–S(5)	2.963(5) × 2		
Ce(2)–S(6)	3.121(6)		
Ce(2)–S(7)	2.897(6) × 2		
Ce(2)–S(8)	2.996(5) × 2		
Rb–S(1)	3.558(4)		
Rb–S(2)	3.395(3) × 2		
Rb–S(3)	3.295(3) × 2		
Rb–S(4)	3.336(4)		
Rb–S(7)	3.378(3) × 2		

$KCe_{1\pm}Bi_{4\pm x}S_8$ (**IV**). A crystal with dimensions $0.65 \times 0.05 \times 0.05$ mm was mounted on a glass fiber and a Rigaku AFC6S four-circle diffractometer equipped with a graphite-crystal monochromator was used for data collection at room temperature. The final cell was calculated from a least-squares refinement using the 2θ angles of 15 carefully centered reflections in the $20^\circ \leq 2\theta \leq 30^\circ$ range. Although data were collected for this compound and the structure was solved, its refinement had several problems. The results were similar to those described above; that is, both high coordinate sites presented the same kind of disorder as in (**I**) and (**III**) but many sulfur atoms were nonpositive definite. Despite this there is no doubt that this compound is isomorphous to (**I**) and (**III**). The final cell, determined from a single crystal, was found to be $a = 16.645(3)$ Å, $b = 4.048(2)$ Å, $c = 21.577(1)$ Å and the space group orthorhombic *Pnma*.

RESULTS AND DISCUSSION

Synthesis and Thermal Analysis

Compounds (**I**) and (**II**) were synthesized by reacting the corresponding alkali metal sulfide, Bi_2S_3 and La_2S_3, in 1:4:1 ratio at temperatures above 800°C. Compounds (**III**) and (**IV**) were synthesized similarly by reacting the corresponding alkali metal sulfide, Bi_2S_3, Ce, and S in a 1 : 4 : 2 : 3 ratio. All compounds melt incongruently between 770 and 880°C, as determined by DTA and powder XRD studies (Table 9). When similar reactions were performed with Cs_2S, instead of K_2S or Rb_2S, a phase with the composition $Cs_{0.7}La_{0.7}Bi_{3.4}S_{5.3}$ (thin needles) was formed which has a different powder pattern from that of the $ALn_{1\pm x}Bi_{4\pm x}S_8$ (A = K, Rb) family and has yet to be characterized (16b). Probably, due to the larger ionic radius of Cs^+, the $ALn_{1\pm x}Bi_{4\pm x}S_8$ structure is not favored and the atoms rearrange to a different structure type.

Although pure products can be obtained by reacting the $A_2S/Bi_2S_3/La_2S_3$ (A = K, Rb) reagents in 1:4:1 ratio (1:4:2:3 when $A_2S/Bi_2S_3/Ce/S$ is used), this structure type also forms from ratios such as 1:3:1 and 1:3:2. In these cases the XRD shows that the $ALn_{1\pm x}Bi_{4\pm x}S_8$ phase is the main product with the presence of some impurity (estimated at 5–10%) peaks which could not be attributed to any known phases.

TABLE 9
Optical Bandgap and Melting Point Data for $ALn_{1\pm x}Bi_{4\pm x}S_8$

Compound	E_g (eV)	m.p. (°C)	Comments
$KLa_{1.28}Bi_{3.72}S_8$	1.0	801	Incongruently
$RbLa_{1\pm x}Bi_{4\pm x}S_8$	1.2	778	Incongruently
$RbCe_{0.84}Bi_{4.16}S_8$	1.1	786	Incongruently
$KCe_{1\pm x}Bi_{4\pm x}S_8$	1.1	772	Incongruently
$KPr_{1\pm x}Bi_{1\pm x}S_8$	1.1	780	Incongruently
$KNd_{1\pm x}Bi_{4\pm x}S_8$	1.1	778	Incongruently

TABLE 10
Single Crystal Unit Cells of $ALn_{1\pm x}Bi_{4\pm x}S_8$

Compound	a (Å)	b (Å)	c (Å)	V (Å^3)
$KLa_{1.28}Bi_{3.72}S_8$	16.6524(9)	4.0712(2)	21.589(1)	1463.6(1)
$KCe_{1\pm x}Bi_{4\pm x}S_8$	16.645(3)	4.048(2)	21.577(1)	1437.7(7)
$KPr_{1\pm x}Bi_{4\pm x}S_8$	16.502(2)	4.0391(5)	21.511(3)	1433.8(4)
$KNd_{1\pm x}Bi_{4\pm x}S_8$	16.462(4)	4.0316(5)	21.503(4)	1427.0(5)
$RbLa_{1\pm x}Bi_{4\pm x}S_8$	16.700(3)	4.078(1)	21.698(5)	1477.6(6)
$RbCe_{0.84}Bi_{4.16}S_8$	16.7469(2)	4.0528(1)	21.753(1)	1476.42(4)

When ratios lower in Bi_2S_3 are used, such as 1:2:1 and 1:1:1, then the $ALn_{1\pm x}Bi_{4\pm x}S_8$ phase is no longer stable and a mixture of products is obtained with the main characteristic being the separation between ternary A–Bi–S phases and binary Ln–S phases. The A–Bi–S phases are β-$KBiS_2$ (isostructural with $RbBiS_2$) and $RbBiS_2$ (4d).

The compounds $KPr_{1\pm x}Bi_{4\pm x}S_8$ and $KNd_{1\pm x}Bi_{4\pm x}S_8$ as well as $KCe_{1\pm x}Bi_{4\pm x}S_8$ and $RbLa_{1\pm x}Bi_{4\pm x}S_8$, are all isostructural and can be synthesized by the same methods described above. Although their structures were not crystallographically refined, the unit cells of these compounds were determined from single crystal samples and are given in Table 10.

Structure

The structure adopted by all compounds is unusual and is made up of NaCl-type and Gd_2S_3-type (22) building blocks which connect to form tunnels filled with alkali metals ions, as shown in Fig. 1. This structure type has three types of metal positions, a six-coordinate site and two sites with higher (> 6) coordination numbers. The NaCl-type fragment contains the six-coordinate positions which are exclusively occupied by Bi atoms, while the Gd_2S_3-type fragment contains the seven- and eight-coordinate positions which display mixed occupancy. The presence of NaCl-type fragments, where Bi has a distorted octahedral coordination, is a common feature in many Bi chalcogenides (11).

A second characteristic of the structure is an infinite rod with a lozenge-like cross section consisting of two columns of monocapped (coordination number 7) and two columns of bicapped (coordination number 8) prisms; see Fig. 2. The monocapped prisms stack into a column by sharing edges, while the bicapped prisms stack by sharing trigonal faces. This arrangement causes the two different kinds of prisms to be disposed perpendicular to each other. This feature occurs in a variety of compounds including Gd_2S_3 (29) , $CeTmS_3$ (30), $La_{10}Er_9S_{27}$(31), $PbBi_2S_4$ (32), $Pb_4In_3Bi_7S_{18}$ (33), and $La_4Bi_2S_9$ (21).

In $KLa_{1.28}Bi_{3.72}S_8$, there is a disorder between Bi and La in the high coordination positions M1 and M2; see Fig. 2A. The seven-coordinate site M1 has a monocapped trigonal

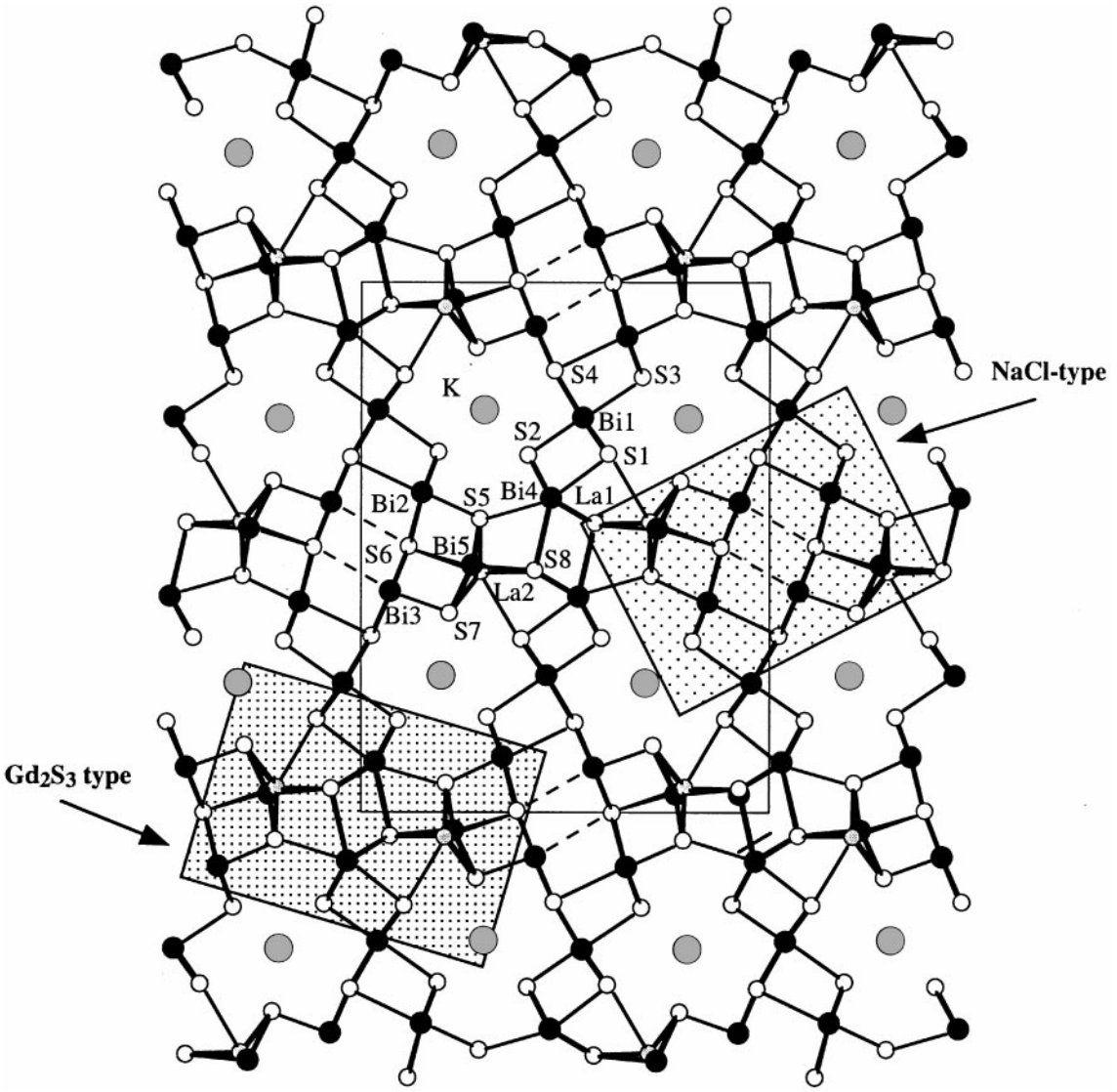

FIG. 1. Projection of the structure of $KLa_{1.28}Bi_{3.72}S_8$ viewed down the *b*-axis. The shaded areas indicate the NaCl-type and Gd_2S_3-type building blocks.

prismatic shape and consists of ~55% Bi (Bi4) and ~45% La (La1). The eight-coordinate M2 site has a bicapped trigonal prismatic shape. The existence of a considerable amount of electron density at a distance of 0.429(6) Å from M2 leads to the resolved splitting of this position into two sites, in which one is ~83% occupied by La (M2, La2) atoms while the other is ~17% occupied by Bi (M2′, Bi5) atoms.

The coordination environments of La^{3+} and Bi^{3+} in the corresponding binary sulfides (La_2S_3 and Bi_2S_3, respectively) have common characteristics, as shown in Fig. 3. As mentioned before in La_2S_3 (Gd_2S_3-type), La atoms exist in monocapped (La1 seven-coordinate) and bicapped (La2 eight-coordinate) trigonal prismatic sites. In Bi_2S_3, one Bi atom (Bi1) has a distorted octahedral coordination and an extra long Bi–S interaction resembling a monocapped trigonal prismatic coordination, while the other Bi (Bi2) has a square pyramidal coordination with three long Bi–S distances (3.32–4.03 Å) resembling a bicapped trigonal prism. The mixed occupancy between Bi and La atoms in $KLa_{1.28}Bi_{3.72}S_8$ can be rationalized based on the similar size and atom arrangements of Bi and La in their binary sulfides. Also in several ternary bismuth chalcogenides, Bi atoms occupy high coordinate sites. For example, in $K_2Bi_8S_{13}$ (13) one bismuth atom occupies a distorted bicapped trigonal prismatic site, disordered with K^+ ions. These sites (which usually are occupied by Bi and other large ions) serve to connect the various structural blocks formed from the octahedrally coordinated Bi atoms. Large ions such as lanthanides can occupy these positions, allowing for some

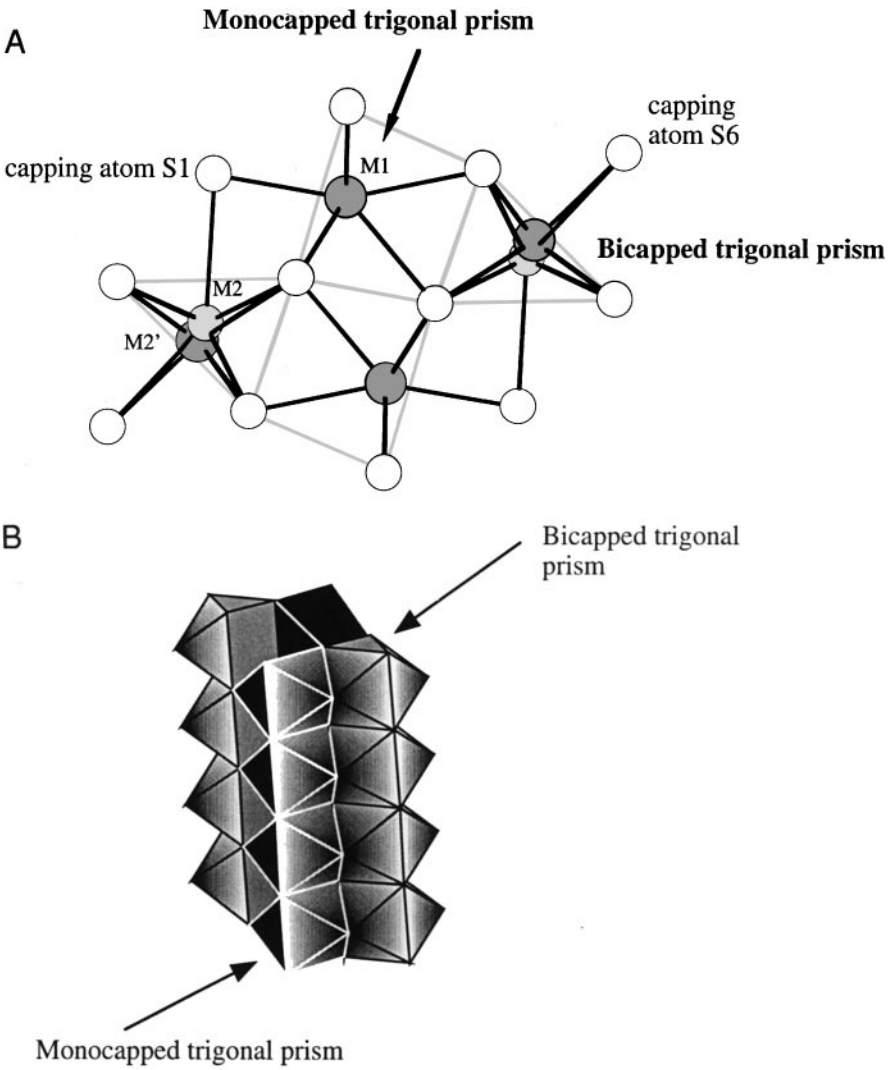

FIG. 2. (A) Orientation of the Gd_2S_3-type infinite rod consisting of two columns of monocapped (coordination number 7) and two columns of bicapped (coordination number 8) prisms. The gray lines show the two different kinds of prisms. (B) Polyhedral view of the prisms as they stack along the *b*-axis. The solid areas indicate the prisms, while the shaded areas show the caps.

interesting substitution chemistry and enabling the potential tuning of the electronic properties of the compounds.

In site M1, the metal–sulfur bonds vary between 2.827(2) and 3.053(3) Å, very close to the values of La(seven-coordinate)–S bonds in La_2S_3 (2.94–3.05 Å). These values are also common for Bi–S bonds. In site M2, the metal–sulfur bonds are in the range 2.940(2)–3.246(4) Å, again very close to the La(eight-coordinate)–S bonds in La_2S_3 (2.91–3.18 Å). Regarding the M2′ site, where the splitting took place, the situation is different. Now there are three short bonds [2.723(8)–2.790(4) Å], one bond at 2.979(4) Å, and three long distances [3.274(6)–3.652(8) Å], and the coordination of the atom resembles more of a square pyramid. Based on the metal–sulfur distances M2 was assigned as La (La2) and M2′ as Bi (Bi5). The coordination of the three octahedral bismuth atoms is also distorted. Characteristic of all Bi atoms is the existence of a long bond *trans* to a short bond. This type of coordination environment is prevalent in bismuth chalcogenides and results from the influence of the stereochemically active $6s^2$ electron lone pair. This distortion is more pronounced for atoms Bi(3) [2.542(3) Å trans to 3.612(3) Å] and Bi(2) [2.563(3) Å trans to 3.257(4) Å]. For all three Bi atoms the bond angles range between ~ 82 and 98°.

$RbCe_{0.84}Bi_{4.16}S_8$ has the same characteristics. The octahedral Bi atoms are distorted, with a long bond trans to a short bond. In site M1 (monocapped trigonal prism) the metal–sulfur bonds vary between 2.827(2) and 3.181(3) Å, and this site consists of 70% Bi and 30% Ce. The other high coordinate (bicapped trigonal prism) position is disordered in the same way as in $KLa_{1.28}Bi_{3.72}S_8$ and consists of 46% Ce (M2, Ce2) and 54% Bi (M2′, Bi5).

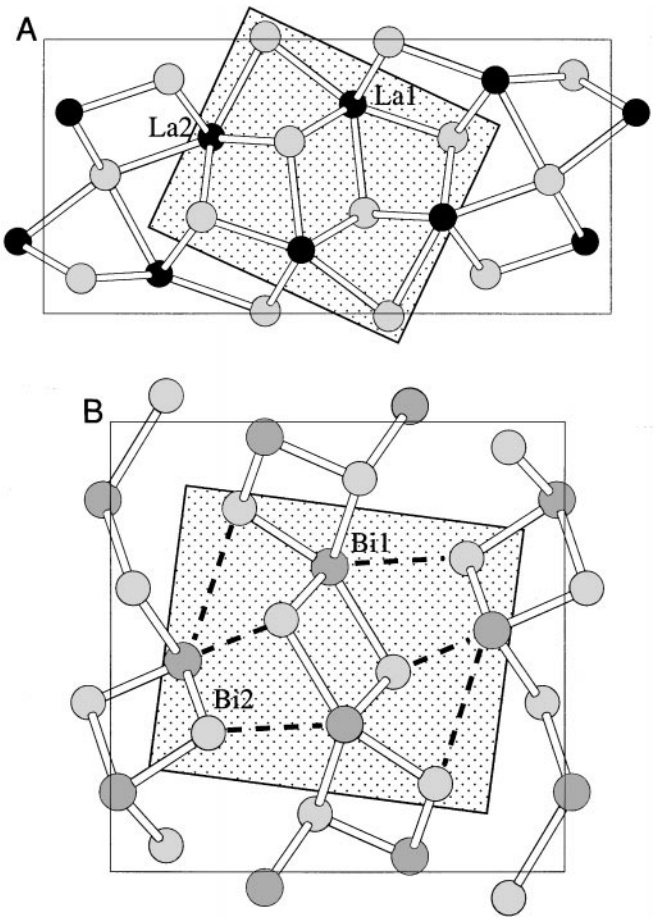

FIG. 3. The structures of La_2S_3 (A) and Bi_2S_3 (B) showing the same Gd_2S_3-type infinite rod found in $KLa_{1.28}Bi_{3.72}S_8$.

The stoichiometry of these compounds is intermediate between two isostructural parent phases of the formula $ALn_2Bi_3S_8$ and ABi_5S_8, none of which has been reported. In $ALn_2Bi_3S_8$ the high coordinate sites are fully occupied by the lanthanide, while in ABi_5S_8 the same sites are occupied by bismuth atoms. As was mentioned before, the similar sizes of Bi^{3+} with La^{3+} and Ce^{3+} and the similar coordination preferences of Bi and Ln result in occupational disorder in the high coordinate sites and produce substantial, entropically favored, deviations from the ideal stoichiometry. In fact, we expect the entire composition range between $ALn_2Bi_3S_8$ and ABi_5S_8 to be accessible under proper experimental conditions.

Remarkably, the compound $Ce_{1.25}Bi_{3.78}S_8$ (22) was reported to have structural characteristics very similar to those of the $ALn_{1\pm x}Bi_{4\pm x}S_8$ compounds presented here. $Ce_{1.25}Bi_{3.78}S_8$ crystallizes in the same orthorhombic space group *Pnma* with a very similar unit cell of $a = 16.55(1)$ Å, $b = 4.053(2)$ Å, $c = 21.52(1)$ Å. The compound was synthesized from a mixture of nominal composition $CeBiS_3$ which was maintained for 15 days under a bath of KCl and KI melted at around 750°C as described by the authors (22). The published fractional atomic coordinates in $Ce_{1.25}Bi_{3.78}S_8$ and the quaternary structures presented in this work are essentially the same. The difference is that the alkali metal site is occupied by Ce which is 1/4 occupied, the M1 site is occupied by 0.78 Bi atoms, and the M2 is occupied fully by Ce. Thus, $Ce_{1.25}Bi_{3.78}S_8$ can be described as $(Ce_{0.25}\square_{0.75})(Ce)(Bi_{0.78}\square_{0.22})Bi_3S_8$, while for comparison $KLa_{1.28}Bi_{3.72}S_8$ can be described as $(K)(Bi_{0.17}La_{0.83})(Bi_{0.55}La_{0.45})Bi_3S_8$. No other analytical data, except for the Bi/Ce ratio, were reported. Furthermore, in order to charge balance $Ce_{1.25}Bi_{3.78}S_8$ one needs the Ce atoms to have a mixed valency of 3+ and 4+; however, the problem of charge balancing was not addressed by the authors. The occurrence of Ce^{4+} in a chalcogenide compound is not only unlikely, given that Ce^{4+} is too oxidizing for sulfide ions, it is also unprecedented. Simple compounds such as CeS_2 are in fact Ce^{3+} systems with S–S bonds in the structure. From the above we conclude that $Ce_{1.25}Bi_{3.78}S_8$ is most likely a $KCe_{1\pm x}Bi_{4\pm x}S_8$ phase, with the K atoms originating from the KCl/KI flux.

Charge Transport Properties and Optical Absorption

Figure 4 shows the electrical conductivity for pressed pellets of the (**I**) and (**II**) compounds. Both compounds are semiconductors with a room temperature conductivity $\sigma \sim 10^{-4}$ S/cm, which drops to 10^{-9} S/cm, at 75 K. These values suggest the presence of a relatively wide bandgap and are in agreement with the optical data which show bandgaps between 1.0 and 1.2 eV (Table 9 and Fig. 5).

Magnetic Properties

The temperature-dependent magnetic susceptibility response of (**III**) is shown in Fig. 6. The compound behaves as a Curie–Weiss paramagnet at high temperature with deviations at low temperatures (< 50 K), caused by crystal field splitting. Above the onset of deviation, a μ_{eff} of 2.31 μ_B and a θ of -43 K were estimated by fitting a straight line to the data. If we take into account that there are 0.84 Ce^{3+} per formula the μ_{eff} is very close to that calculated 2.13 μ_B for the free ion (34). (**IV**) behaves in a similar way (Curie–Weiss paramagnet) with a μ_{eff} of 2.34 μ_B and a θ of -61 K. The magnetic response of the (**I**) and (**II**) was not investigated, since La^{3+} is an f^0 cation and is expected to be diamagnetic. The magnetic properties of (**V**) and (**VI**) were not studied.

CONCLUDING REMARKS

The family of phases of the type $ALn_{1\pm x}Bi_{4\pm x}S_8$ with La, Ce, Pr, and Nd adopts a structure type which consist of Gd_2S_3-type and NaCl-type fragments. The fragments connect to form tunnels in which the alkali metals reside. In the

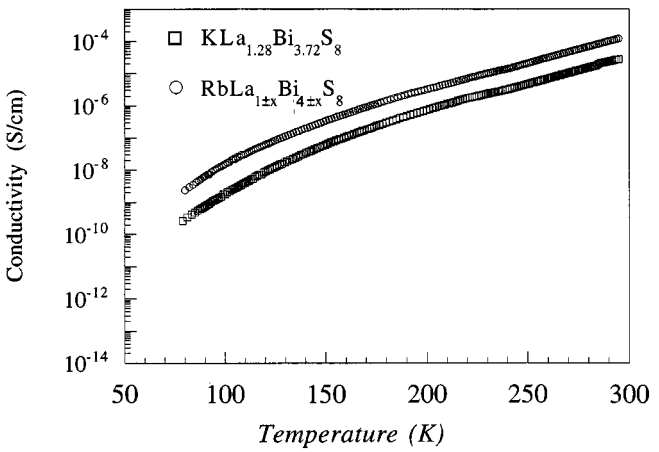

FIG. 4. Variable temperature electrical conductivity for pressed pellets of $KLa_{1.28}Bi_{3.72}S_8$ and $RbLa_{1\pm x}Bi_{4\pm x}S_8$.

seven and eight-coordinate sites in the structure there is a mixed occupancy between the lanthanide and the bismuth atoms which derives from the similar size of these atoms. All compounds are semiconductors with bandgaps around 1.0 eV and the La compounds show a room conductivity of

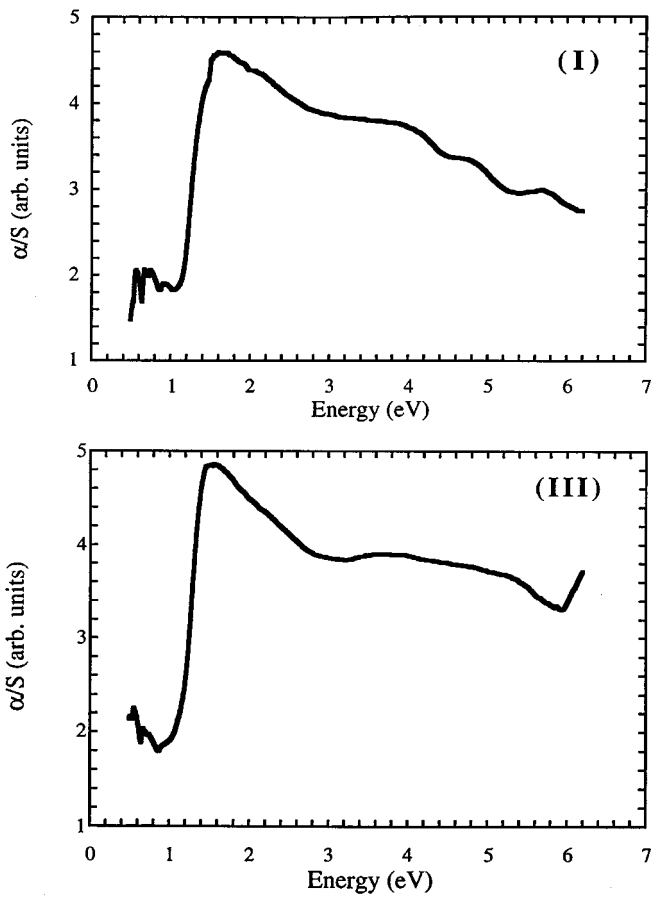

FIG. 5. Solid state UV/Vis spectra of $KLa_{1.28}Bi_{3.72}S_8$ (**I**) and $RbCe_{0.84}Bi_{4.16}S_8$ (**III**).

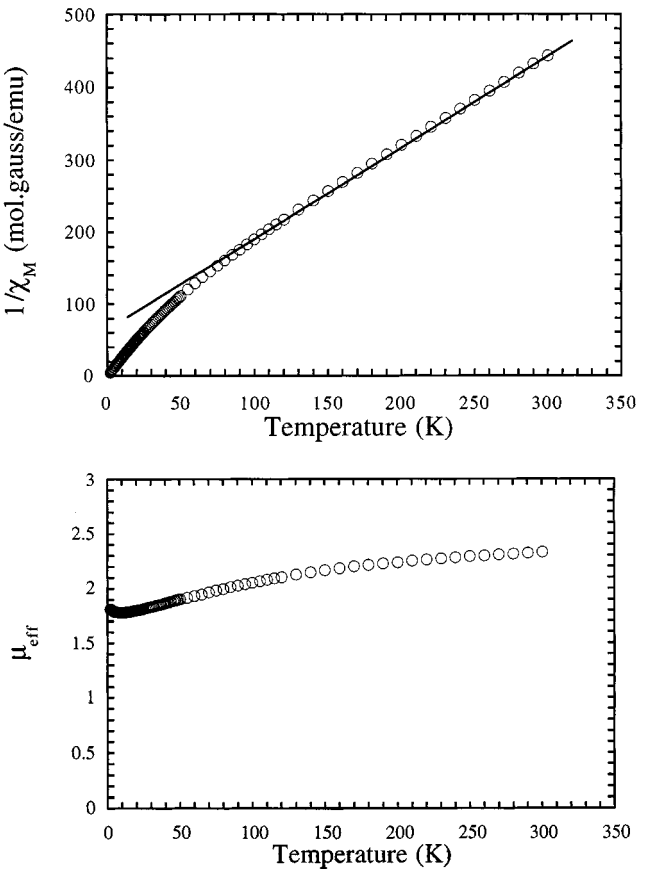

FIG. 6. (Top) Inverse magnetic susceptibility $1/\chi_m$ plotted against temperature for $RbCe_{0.84}Bi_{4.16}S_8$. (Bottom) Effective magnetic moment vs temperature for $RbCe_{0.84}Bi_{4.16}S_8$.

10^{-4} S/cm. The electrical conductivities are too small for room temperature thermoelectric applications. In order to increase the conductivity, the bandgaps should be decreased and this could be attempted by working with the corresponding Se systems.

ACKNOWLEDGMENTS

Financial support from the Office of Naval Research (Contract N00014-98-1-0443) is gratefully acknowledged. This work made use of the SEM facilities of the Center for Electron Optics at Michigan State University. The Siemens SMART platform CCD diffractometer at Michigan State University was purchased with funds from the National Science Foundation (CHE-9634638). At Northwestern University this work made use of Central Facilities supported by NSF through the Materials Research Center (DMR-96-32472). The authors thank Victor G. Young and the X-Ray Crystallographic Laboratory of the University of Minnesota for collecting the X-ray data set of (**III**).

REFERENCES

1. (a) E. Mackovicky, *Fortschr. Miner.* **59,** 137 (1981); (b) E. Mackovicky, *Fortschr. Miner.* **63,** 45 (1985); (c) E. Mackovicky, *Z. Kristallogr.* **173,** 1 (1985); (d) E. Mackovicky, *N. Jb. Mineral. Abh.* **160,** 269 (1989); (e) E. Mackovicky, E. *Eur. J. Mineral.* **5,** 545 (1993).

2. (a) M. G. Kanatzidis, T. J. McCarthy, T. A. Tanzer, L.-H. Chen, T. Hogan, C. R. Kannewurf, and L. Iordanidis, *Mat. Res. Soc. Symp.* **410,** 37 (1996); (b) D.-Y. Chung, T. Hogan, J. L. Schindler, L. Iordanidis, W. Brazis, C. R. Kannewurf, B. Chen, C. Uher, and M. G. Kanatzidis, *Mat. Res. Soc. Symp.* **478,** 333 (1997).
3. (a) H.-H. Jeon, H.-P. Ha, D.B. Hyun, and J.-D. Shim, *J. Phys. Chem. Solids* **4,** 579 (1991); (b) L. R. Testardi, J. N. Bierly, Jr., and F. J. Donahoe, *J. Phys. Chem. Solids* **23,** 1209 (1962); (c) C. H. Champness, P. T. Chiang, P. Parekh, *Can. J. Phys.* **43,** 653 (1965); (d) **45,** 3611 (1967).
4. (a) J. W. Boon, *Rec Trav. Chim. Pays-Bas* **63,** 32 (1944); (b) O. Glemser, and M. Z. Filcek, *Anorg. Allg. Chem.* **279,** 321 (1955); (c) G. Gattow, and J. Z. Zemann, *Z. Anorg. Allg. Chem.* **279,** 324 (1955); (d) Y. V. Voroshilov, E. Y. Peresh, and M. I. Golovei, *Inorganic Materials* **8,** 777 (1972).
5. A. S. Kanischeva, J. N. Mikhailov, V. B. Lasarev, and A. F. Trippel, *Dokl. Akad. Nauk., SSSR* (*Kryst.*) **252,** 96 (1980).
6. D. Schmitz, and W. Bronger, *Z. Naturforsch.* **29b,** 438 (1974).
7. G. Cordier, H. Schäfer, and C. Schwidetzky, *Rev. Chim. Miner.* **22,** 676 (1985).
8. B. Aurivillus, *Acta Chem. Scand. A* **37,** 399 (1983).
9. G. Cordier, H. Schäfer, and C. Schwidetzky, *Rev. Chim. Miner.* **22,** 631 (1985).
10. K. Volk, G. Cordier, R. Cook, and H. Z. Schäfer, *Naturforsch.* **35b,** 136 (1980).
11. T. J. McCarthy, S.-P. Ngeyi, J.-H. Liao, D. DeGroot, T. Hogan, C. R. Kannewurf, and M. G. Kanatzidis, *Chem. Mater.* **5,** 331 (1993).
12. T. J. McCarthy, T. A. Tanzer, and M. G. Kanatzidis, *J. Am. Chem. Soc.* **117,** 1294 (1995).
13. (a) M. G. Kanatzidis, T. J. McCarthy, T. A. Tanzer, L.-H. Chen, L. Iordanidis, T. Hogan, C. R. Kannewurf, C. Uher, and B. Chen, *Chem. Mater.* **8,** 1465 (1996); (b) B. Chen, C. Uher, L. Iordanidis, and M. G. Kanatzidis, *Chem. Mater.* **9,** 1655 (1997).
14. D.-Y. Chung, K.-S. Choi, L. Iordanidis, M. G. Kanatzidis, J. L. Schindler, W. Brazis, C. R. Kannewurf, B. Chen, S. Hu, and C. Uher, *Chem. Mater.* **9,** 3060 (1997).
15. D.-Y. Chung, S. Jobic, T. Hogan, C. R. Kannewurf, R. Brec, R. Rouxel, and M. G. Kanatzidis, *J. Am. Chem. Soc.* **119,** 2505 (1997).
16. (a) L. Iordanidis and M. G. Kanatzidis, manuscript in preparation; (b) L. Iordanidis and M. G. Kanatzidis, work in progress.
17. W. Choe, S. Lee, P. O'Connell, and A. Covey, *Chem. Mater.* **9,** 2025 (1997).
18. M. G. Kanatzidis and F. J. DiSalvo, *Nav. Res. Rev.* **4,** 14 (1996).
19. P. Lemoine, D. Carre, and M. Guittard, *Acta Cryst. C* **42,** 259 (1986).
20. P. Lemoine, D. Carre, and M. Guittard, *Acta Cryst. B* **38,** 727 (1981).
21. C. Ecrepont, M. Guittard, and J. Flauhaut, *Mat. Res. Bull.* **23,** 37 (1988).
22. R. Ceolin, P. Toffoli, P. Khodadad, and N. Rodier, *Acta Cryst. B* **33,** 2804 (1977).
23. O. M. Aliev, T. F. Maksudova, N. D. Samsonova, L. D. Finkel'shtein, and P. G. Rustamov, *Inorganic Materials* **22,** 23 (1986).
24. K.-S. Choi, L. Iordanidis, K. Chondroudis, and M. G. Kanatzidis, *Inorg. Chem.* **36,** 3804 (1997).
25. E. A. Axtell, III, J.-H. Liao, Z. Pikramenou, and M. G. Kanatzidis, *Chem. Eur. J.* **2,** 656 (1996).
26. (a) T. J. McCarthy, S.-P. Ngeyi, J.-H. Liao, D. DeGroot, T. Hogan, C. R. Kannewurf, and M. G. Kanatzidis, *Chem. Mater.* **5,** 331 (1993); (b) J. W. Lyding, H. O. Marcy, T. J. Marks, and C. R. Kannewurf, *IEEE Trans. Instrum. Meas.* **37,** 76 (1988).
27. CERIUS^2, Version 1.6, Molecular Simulations, Inc. Cambridge, England, 1994.
28. (a) SMART, Siemens Analytical X-ray Systems Inc., Madison, Wisconsin, 1996; (b) SAINT V-4, Siemens Analytical X-ray Systems, Inc., Madison, Wisconsin, (1994–1996); (c) G. M. Sheldrick, University of Göttingen, Germany; (d) SHELXTL V-5, Siemens Analytical X-ray Systems, Inc., Madison, Wisconsin.
29. C. T. Prewitt, and A. W. Sleight, *Inorg. Chem.* **7,** 1090 (1968).
30. N. Rodier, *Bull. Soc. Fr. Mineral. Cristallogr.* **96,** 350 (1973).
31. D. Carre and P. Laruelle, *Acta Cryst.* **29,** 70 (1973).
32. Y. Iitaka and W. Nowacki, *Acta Cryst.* **15,** 691 (1962).
33. V. Kramer and I. Reis, *Acta Cryst. C* **42,** 249 (1986).
34. N. N. Greenwood and A. Earnshaw, "Chemistry of the Elements," p. 1443, Pergamon Press, New York, 1984.